SIAM J. Applied Dynamical Systems
Vol. 10, No. 4, pp. 1213–1231

Collective Behaviors in Two-Dimensional Systems of Interacting Particles*

Joceline Lega†

Abstract. This article presents results of molecular dynamics simulations that show the emergence of collective behaviors in a two-dimensional system of particles (hard disks) interacting through a properly chosen collision rule. The particles, which are of finite size and are in free flight between collisions, are not self-propelled. They tumble randomly like bacteria and interact only when they collide, not through continuous potential forces. This work therefore indicates that interactions at the microscopic level, which occur only locally and discretely both in time and space, are sufficient to lead to large-scale macroscopic behaviors. Order parameters that capture and quantify the formation of collective behaviors are introduced and used to describe how the choice of collision rule affects the steady state dynamics of the system, by comparing the outcome to the standard case of elastic collisions. This work was motivated by recent results on the dynamics of bacterial colonies. Possible applications of the present approach to other systems are also discussed.

Key words. interacting particles, bacterial colonies, molecular dynamics simulations, collective behaviors, multiscale systems

AMS subject classifications. 92-08, 92B99, 70F99, 34C28

DOI. 10.1137/100817449

1. Introduction.

Understanding animal aggregation [1, 2] or grouping [3], such as the formation of flocks [4], locust swarms [5, 6], herds [7], or fish schools [8], has always been a fascinating question. The emergence of collective behaviors raises not only ecological questions (concerning the purpose, formation, and functionality of a group) but also modeling challenges (such as identifying the mechanisms behind the formation and persistence of a group) [9]. Models written at the scale of individual agents typically consist of a collection of overdamped stochastic classical (Newton) equations of motion. Each group member propels itself, feels attractive and repulsive forces exerted by other members, often tends to align its direction of motion with the average direction of its neighbors, and may also be subject to drag and to random forces [3, 10, 11, 12, 13]. Some models include the effect of the environment [14] as well as the presence of leaders [15, 16].

These models are independent of scale in the sense that the above principles of self-propulsion, stochasticity, attraction, repulsion, alignment, etc. apply from the macroscopic scale of animal herds or pedestrian flow [17] to the microscopic scale of bacteria [12] (assuming the latter communicate, for instance, through chemotaxis or long-range hydrodynamic interactions [18]). In 1995, Vicsek et al. [19] introduced a simple model for the interaction of self-propelled particles, in which each particle moves at constant speed and ad-

*Received by the editors December 8, 2010; accepted for publication (in revised form) by L. Fauci August 16, 2011; published electronically October 4, 2011. This research was supported by the National Science Foundation under grant 0405551.
http://www.siam.org/journals/siads/10-4/81744.html
†Department of Mathematics, University of Arizona, 617 N. Santa Rita Avenue, Tucson, AZ 85721 (lega@math.arizona.edu).

justs its direction of motion according to the average velocity field of its neighbors, up to some additive noise. They showed that a phase transition occurs as the density of particles increases (or the noise decreases), corresponding to the appearance of collective behaviors (that is, a global, nonzero average velocity of the group). There is now an abundant literature on the dynamics of collections of self-propelled or *active Brownian* particles [20, 21, 22, 23, 24, 25, 26, 27, 28, 29, 30, 31, 32]. Many of these models assume an overdamped situation in which friction with the external medium is dominant, so that the velocity of each particle can be expressed as a sum of deterministic and/or stochastic forces. Others use the complete Newton equations but introduce a velocity-dependent friction [23], which can therefore account for self-propulsion. They all illustrate the formation of collective motions and, in some cases [20, 21, 22, 23, 29, 30, 31], also reproduce vortex or milling structures. Similar models are used to describe groups of autonomous unmanned vehicles [33, 34, 35, 36, 37] or the dynamics of colloidal particles in a fluid [38, 39], and to simulate flocking behavior in computer animations [40]. More recently, studies that involve self-propelled rods or needles have shown that elongated body shapes facilitate aggregation [41].

This approach, which often relies on potential (i.e., gradient-like) attractive and repulsive interactions, assumes some level of communication (for instance, through visual, electrostatic, or chemical cues) between the agents. However, collective motions have also been observed [42] (see [43] as well) in systems of bacteria which grow on agar, do not produce wastes or surfactants, and therefore do not appear to communicate with one another. In such a case, the only mode of interaction between agents is likely to be through some form of physical contact, possibly mediated by the medium in which they move. The bacterial density is indeed very high in these systems, and if hydrodynamic interactions play a role in such situations, their cumulative effect is probably short ranged. Since such interactions are local in time and space, they may be considered as "generalized collisions." Because the latter do not have to conserve momentum or energy, they are, however, more general than elastic collisions between molecules in gases or liquids, or inelastic collisions in granular media (for a review on the dynamics of granular gases, see, for instance, [44]). It is known that inelastic collisions (which dissipate energy) favor clustering [45, 46]. It was moreover suggested in [46] that "the averaging of velocity directions in the Vicsek model can be compared locally to the cooling of a granular medium," and shown that a gas of self-propelled particles undergoing inelastic collisions can self-organize into vortex structures [46]. Simulations of collections of self-propelled needles that interact through volume exclusion [41, 47] have shown that this simple constraint forces the needles to align locally and create structures in the form of large-scale jets, at the size of the system [47].

It is therefore legitimate to ask whether it is possible to find (generalized) collision rules between particles at the microscopic level that can lead to the creation of coherent structures at the macroscopic level. The goal of this paper is to present numerical results that suggest the answer is yes. More precisely, we have run molecular dynamics simulations of hard disks that interact through a given collision rule (described by (2.1)) and that randomly tumble [48, 49], like bacteria. The resulting dynamics differs significantly from the behavior that would be observed with elastic collisions, which typically lead to chaotic dynamics. These differences are quantified through various measures of order and clustering in section 3. The rest of this article is organized as follows. Section 2 describes the chosen collision rule and the numerical

method used. Possible reasons for the emergence of collective behaviors in systems of colliding particles, as well as possible ways of establishing appropriate collision rules, are given in section 4. Finally, section 5 presents various directions in which this work could be continued. In particular, links with complex systems and macroscopic models are discussed.

2. Numerical simulations. We perform simulations of $N = p^2$ disk-like particles in a square box of side length L, with periodic boundary conditions. The radius ρ of each disk depends on the packing fraction η of the system. The latter is the only relevant parameter in the simulation and is related to ρ by

$$\eta = \frac{N\pi\rho^2}{L^2} \Longrightarrow \rho = \sqrt{\frac{L^2\eta}{N\pi}}.$$

2.1. Collision rule. Between collisions, particles are in free flight and move with a constant velocity. When two particles collide, their velocities $\vec{u}_1$ and $\vec{u}_2$ after the collision are given, in terms of their velocities $\vec{v}_1$ and $\vec{v}_2$ entering the collision, by the following map:

$$\begin{aligned}
&(\vec{v}_1, \vec{v}_2) \mapsto (\vec{u}_1, \vec{u}_2), \quad \vec{u}_1 = \frac{1}{2}\left(\vec{v}_1 + \vec{v}_2 + \alpha\,\delta\vec{v}\right), \quad \vec{u}_2 = \frac{1}{2}\left(\vec{v}_1 + \vec{v}_2 - \alpha\,\delta\vec{v}\right), \\
&\delta\vec{v} = \frac{\vec{v}\cdot\vec{r}}{||\vec{r}||^2}\,\vec{r}, \qquad \vec{r} = \vec{r}_2 - \vec{r}_1, \qquad \vec{v} = \vec{v}_2 - \vec{v}_1, \\
&\alpha = \frac{||\vec{v}||}{||\delta\vec{v}||} \qquad \text{if } ||\delta\vec{v}|| \neq 0 \quad \text{and} \quad \alpha = 0 \text{ otherwise.}
\end{aligned} \tag{2.1}$$

For comparison, a binary elastic collision, which conserves momentum and kinetic energy, is given by

$$(\vec{v}_1, \vec{v}_2) \mapsto (\vec{u}_1, \vec{u}_2), \qquad \vec{u}_1 = \vec{v}_1 + \delta\vec{v}, \qquad \vec{u}_2 = \vec{v}_2 - \delta\vec{v}, \tag{2.2}$$

where $\delta\vec{v}$, $\vec{r}$, and $\vec{v}$ are defined as above. In this case, the velocities in the frame moving with the center of mass of the two particles are such that their components parallel to the vertical collision plane (i.e., perpendicular to $\vec{r}$) are unchanged, while their perpendicular components are reversed by the collision. The collision map given by (2.1), which is for a two-dimensional system, was chosen as an interpolation between the statement that "Colliding bacteria ... swimming from left to right begin misaligned, reorient during collision, and swim off parallel afterwards" made in [50] and the statement that "parallel swimming motion of bacteria is unstable and breaks down easily in three dimensions" made in [51]. Collision rule (2.1) conserves energy if $\alpha \neq 0$. If $\delta\vec{v} = \vec{0}$, that is, in the case of a grazing collision, the two particles have identical velocities after the collision. Otherwise, their postcollision velocities differ by $\alpha\delta\vec{v}$. At this point, there is little information in the experimental or theoretical literature on the exact nature of the interaction between bacteria, and the choice of the above collision rule is somewhat ad hoc. It could, however, be informed in the future by theoretical works which seek to establish how two bacteria moving in a Stokes flow affect one another, as is done, for instance, in [51] for spherical particles with one flagellum. Moreover, simulations of large collections of interacting slender bodies, such as in [52], could be revisited in the context of the present work, provided that a collision rule can be established for the pushers

and pullers that are considered in that work. For instance, the correlation plots of [52] show that pushers close to one another tend to swim in the same direction, whereas "nearby pullers are likely to be misaligned and swimming in opposite directions," and such statements could be used to define a collision rule for these types of swimmers. It would then be interesting to see how the dynamics resulting from such local collisions compares to the behaviors reported in [52], which are based on long-range hydrodynamic interactions. The main point of this article, however, is to illustrate the fact that some collision rules can give rise to clustering and large-scale structures, and the map (2.1) provides such an example.

We include only binary collisions in the simulation. If more than two particles happen to collide at the same time, then the code first processes a binary collision between two of the colliding particles. A collision occurs only if the particles are in contact (i.e., the distances between their centers of mass is equal to their diameter) and if their velocities are such that the particles are moving toward one another, i.e., if $\vec{v}\cdot\vec{r} \leq 0$, with grazing collisions corresponding to $\vec{v}\cdot\vec{r} = 0$. Thus, after the code has processed a binary collision between two of the particles involved in a tertiary or higher order collision, it is possible that the directions of the velocities of these particles are now such that they do not appear to collide with any of the remaining particles. If they do, however, the code selects two of the particles that are flagged as colliding and proceeds as before. It should also be noted that it is possible, especially in the case where $\vec{v}$ and $\vec{r}$ are parallel to one another, for particles to overlap after a collision given by (2.1). However, this is very infrequent in normal regimes, and we use the Morisita index [53] (see section 3.4) to detect the presence of such events in the simulations. In all of the runs presented here, the particles never overlap.

2.2. Cell structure, head table, and linked list. In order to simulate large numbers of interacting particles in reasonable time, the codes make use of memory- and time-saving techniques typical of molecular dynamics simulations [54, 55, 56]. Such methods, which rely on *cell structures* and *linked lists*, make it possible to simulate systems of hundreds of finite-size particles in manageable time. The need for such a tool is easy to understand: imagine a system of hard disks in which particles move at constant velocity between consecutive collisions. Most of the computation time is spent calculating collision times between all of the particles in the system. For a large number of particles, this can be extremely demanding. If the simulation box is instead divided into a collection of smaller *cells*, this time is considerably reduced since one need only look at particles in the same or adjacent cells when computing collision times (assuming the cells are not too small or the speed of the particles is not too fast). The extra cost is in keeping track of the cells that each particle visits, and of the particles that are in each of the cells. This can be accomplished in a way that economizes memory space by creating a *head table* and a *linked list*. The former keeps track of whether a cell is occupied or not, and if it is, points to the latter, which links all of the particles in a given cell. A performance study of the codes used in this work shows that the computation time decays faster than exponentially as the number of cells in the box is increased. Of course, cells cannot be too small, so for each number of particles, there is a range of acceptable numbers of cells that optimize between the gain in computing a smaller number of collision times and the added expense of tracking particles as they move between cells.

The use of a head table and a linked list makes it easy to find all of the particles in a given cell and to update these matrices when a particle moves from one cell to another. The "head

matrix" `head` is a table of length equal to the number of cells, such that the jth entry of `head` is the index of a particle in cell j. If that cell is empty, then $\texttt{head}(j) = 0$. The entries of the matrix `list` are such that $\texttt{list}(j) = i$ means that particle i is in the same cell as particle j, and $\texttt{list}(j) = 0$ means that there are no other particles in that cell. To illustrate how this works, assume, for instance, that one needs to find all of the particles in cell c. The first step is to look at $\texttt{head}(c)$. If $\texttt{head}(c) = 0$, then there are no particles in cell c. If not, $\texttt{head}(c) = j_1$, where j_1 is the index of one of the particles in the cell. One then looks at $\texttt{list}(j_1)$. If it is zero, then particle j_1 is alone in cell c. If not, $\texttt{list}(j_1) = j_2$ and j_2 is the index of another particle in cell c. One then looks at $\texttt{list}(j_2) = j_3$. If $j_3 = 0$, then cell c contains only two particles of indexes j_1 and j_2. If not, then particle j_3 is also in cell c, and one then needs to look at $\texttt{list}(j_3) = j_4$. This process is repeated until $\texttt{list}(j_k) = 0$, which means that cell c contains k particles and that particle k is the "last" particle in that cell.

2.3. Initial conditions, advance in time, and simulation output. The simulation keeps track of the following information for each particle: its x and y coordinates, the components v_x and v_y of its velocity vector, the index of the cell it is in, its next tumbling time, its next collision time, the index of the particle it will collide with next, the time at which it will exit its current cell, the index of the cell it will visit next, the time at which its position was last updated,[1] the values L_x and L_y (which are multiples of L and could be positive or negative) to be added to the x and y coordinates of the particle to calculate the position it would have if it were not bound to a system with periodic boundary conditions, and by how much L_x and L_y should be changed when the particle enters the cell it will visit next.

The initial conditions are such that the particles are placed at the nodes of a square lattice and given a random velocity, according to a Maxwellian distribution (each of the components of the velocity vector satisfies a Gaussian distribution of zero mean and variance $\sigma^2 = T_0$, where T_0 is the initial temperature of the system). The velocities are chosen so that the total momentum of the system is zero. If the collisions are elastic, T, which represents the total kinetic energy, is conserved. Collision rule (2.1), however, does not conserve energy, since α may be zero if $\vec{v} = \vec{0}$ or, more likely, $\delta\vec{v} = \vec{0}$. As a consequence, T initially decreases as a function of time. However, because these simulations are supposed to model bacterial systems, each particle is set to spontaneously change its direction of motion and its speed randomly in time. Such events are similar to bacterial tumbles [48], and, if there were no collisions, each particle would move by a succession of runs (motion along a straight line at constant speed) and tumbles, thereby performing a random walk on the plane [49]. After a "tumble," each particle in the simulation has a velocity vector whose direction is random (the angle with an axis of reference is uniformly distributed on $[0,\ 2\pi]$) and whose magnitude is given by the Maxwellian associated with the initial temperature $T_0 > T$. As a consequence, energy is put back into the system by the random tumbling events, and the system eventually equilibrates around a temperature which is nonzero. Times between consecutive tumbles of a particle are uniformly distributed on the interval $[0, 1]$ in all of the simulations shown below. The code is designed to properly handle situations where a tumble occurs on the boundary of the numerical box or on that of a cell inside the domain of simulation.

[1] In order to save time, the position of a particle is updated only when it is necessary, that is, when the particle tumbles or collides with another particle.

Advance in time is performed as follows. At the beginning of the simulation, once the initial positions and velocities are known, one determines the times at which each particle will first enter into a collision, tumble, and exit its cell. It is then easy to determine when the first event (a particle exits its cell or tumbles, or two particles collide) will occur. To process this event, one needs to update the speeds of the particle(s) involved in the event, and update its/their collision times, as well as the collision times of all of the particles that were to collide with the particle(s) that have changed speed. Once this is done, the time at which the next event occurs is calculated, and the process is repeated until the end of the simulation. Between events, particles move at constant speed on a straight line path, and therefore one can exactly calculate the position of any of them at any time if needed. An event involves only one or two particles, and therefore requires a small number of operations to be processed. In particular, because it is not necessary to know where all of the particles are in order to process, say, the collision between two particles, one can actually simulate a very large number of events in a reasonable time. In other words, the simulation is relatively fast because all of the events are local in nature.

The output of each simulation is a list of all of the times at which a collision occurred, together with a complete status of the system at these times. During the postprocessing phase of the simulation, one can use this information to reconstruct the dynamics of the system of interacting particles and determine relevant statistics. Even though the particles are treated as identical disks of radius ρ in the simulations, they are represented as rod-like objects in the snapshots and animations shown in this paper. Each rod is parallel to the velocity vector of the particle it represents and has a length equal to its diameter, 2ρ. This way of presenting the results has the advantage of combining information on the size and direction of motion of a disk-like object into only one element, a rod.

Videos were created with the MATLAB `movie2avi` routine and then downsized and converted to QuickTime format with Adobe Premiere Elements 4.0.

3. Results. Figure 1 shows snapshots at $t = 65$ of a system with $N = 25^2$ particles, with packing fractions $\eta = 0.15$, $\eta = 0.45$, and $\eta = 0.60$. The collision rule is given by (2.1). Recall that the particles are disks and not points. In each picture, a particle is represented by a rod of length equal to the diameter of each disk and parallel to the direction of the velocity vector of the corresponding particle. Two facts are visible from these pictures: (i) the particles tend to cluster, and (ii) the size of the clusters increases with the packing fraction. For comparison, Figure 2 shows similar snapshots for a system with elastic collisions. The difference is already visible in the still pictures but is more striking in the movies, where the eye can easily pick up spatial and temporal correlations: in the case of elastic collisions, where the dynamics is chaotic, no clustering is observed. The following sections introduce a few measurable quantities that help quantify the above statements as well as the difference in behavior between elastic collisions and the collision rule given by (2.1).

3.1. Geometric order parameter. We will say that the system is *ordered* if all of the particles have the same number of neighbors. For disk-like particles, a perfectly ordered arrangement is given by a hexagonal packing of the particles. In this case, each particle has exactly six neighbors. We therefore define, as an order parameter, the probability that a particle has exactly six neighbors. This definition makes sense only if such a probability is a well-defined characteristic of the system.

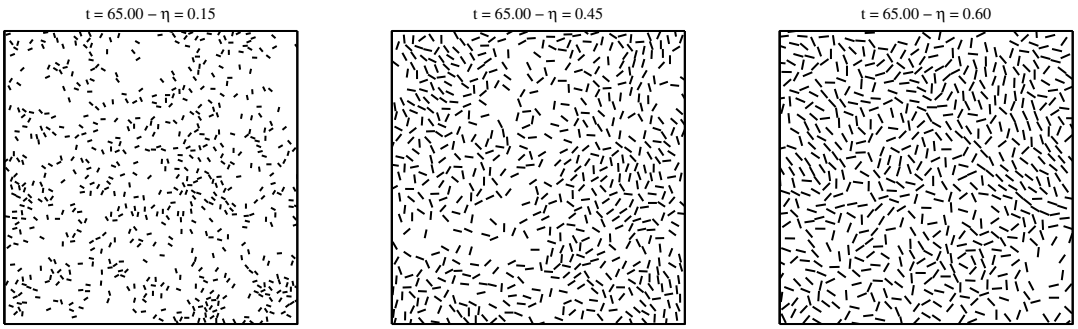

Figure 1. *Snapshots at* $t = 65$ *of a system of* 625 *disk-like particles undergoing collisions described by* (2.1)*, at different packing fractions* η*. The numerical box is a square with periodic boundary conditions and was subdivided into* 15^2 *square cells. The particles are represented by rods going through their center, parallel to the direction of their velocity vector, and of length equal to their diameter. Left:* $\eta = 0.15$*; middle:* $\eta = 0.45$*; right:* $\eta = 0.60$*. See the accompanying movie files* 81744_01.mov [local/web 6.17MB]*,* 81744_02.mov [local/web 7.82MB]*, and* 81744_03.mov [local/web 8.33MB].

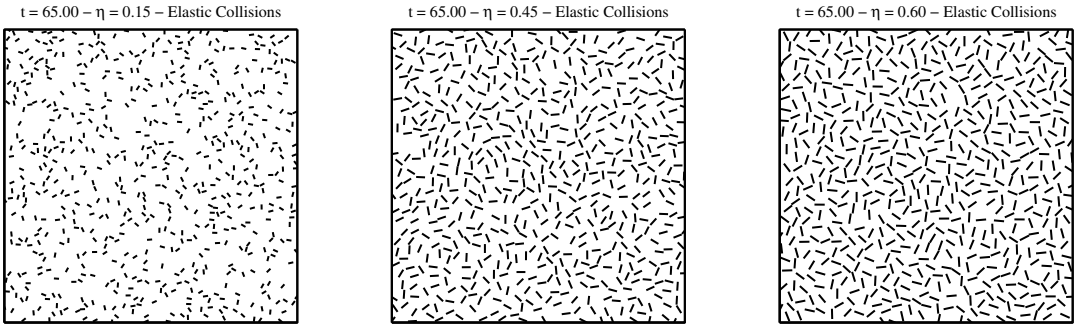

Figure 2. *Same as Figure* 1*, but for elastic collisions. See the accompanying movie files* 81744_04.mov [local/web 6.66MB]*,* 81744_05.mov [local/web 8.29MB]*, and* 81744_06.mov [local/web 8.73MB].

At any given time, it is possible to count the number of neighbors of each particle by performing a Voronoi tessellation of the numerical box. Voronoi cells have the following properties: they are polygonal and form a partition of the numerical box; each Voronoi cell contains only one particle; and each side of a Voronoi cell is placed halfway between the particle in the cell and one of its nearest neighbors and is perpendicular to the line segment joining these two particles. As a consequence, the number of sides of a Voronoi cell is equal to the number of nearest neighbors of the particle in that cell. Figure 3 shows Voronoi tessellations for the snapshots in Figure 1. The color of each cell indicates the number n of its sides or, equivalently, its number of neighbors. Clusters correspond to small Voronoi cells, and regions of low particle density are associated with larger Voronoi cells. At any time t, one can use the Voronoi tessellation to estimate the corresponding distribution of neighbors and define an instantaneous order parameter $A(t)$ by

$$A(t) = P(t, 6),$$

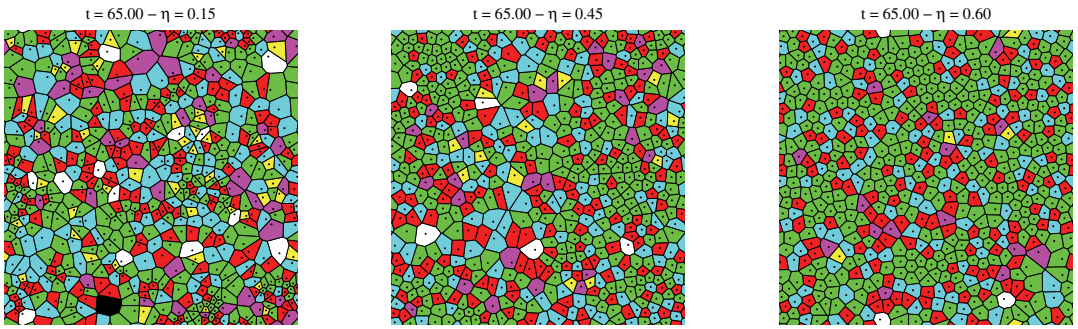

Figure 3. *Voronoi tessellations of the snapshots shown in Figure 1. Green cells have six neighbors, red ones have five, and blue ones have seven. Note the increase in the number of penta-hepta (red-blue) pairs as the system organizes itself into a regular lattice (a perfect lattice would have only green cells).*

where $P(t,n)$ is the probability for a particle to have n neighbors, at time t. For a given simulation, the quantity $A(t)$ of course fluctuates in time but has very small variance when the dynamics reaches steady state. Its mean,

$$A = \langle A(t) \rangle,$$

where $\langle \cdot \rangle$ denotes time averaging, is thus a good characteristic of the system. Since $P(t,n)$ has small fluctuations, one also can define, for a given value of η, a discrete distribution function $P(n)$, which gives the probability that a particle has n neighbors at any time in the steady state regime of the dynamics. Since the number of particles is constant, the parameter $A = \langle A(t) \rangle$ may also be obtained from the distribution of neighbors $P(n)$ in the steady state regime of the dynamics, and is given by $A = P(6)$. Figure 4 shows the numerically evaluated discrete probability distribution function P for $\eta = 0.15$, $\eta = 0.45$, and $\eta = 0.60$. The respective values of A are given in the caption. By definition, A is invariant under translations and rotations, and is therefore a good geometric order parameter.

In two-dimensional systems of hard disks undergoing elastic collisions, a phase transition between the liquid and solid phases occurs between $\eta = 0.706$ and $\eta = 0.910$. This transition is believed to be mediated by dislocations corresponding to penta-hepta pairs (which are pairs of particles, one with five and one with seven neighbors) [57, 58, 59, 60]. In the solid state, the particles are arranged on a hexagonal lattice and vibrate about their mean position. In what follows, we choose values of η less than or equal to 0.6, to stay away from the liquid-solid transition. In Figure 3, cells with five neighbors are colored in red, those with six in green, and those with seven in light blue. Note that as the packing fraction η increases, regions with hexagonal (green) arrangements become more frequent and are separated by penta-hepta (red-blue) pairs. In other words, the transition toward densely packed arrangements in a system with collisions given by (2.1) also appears to be mediated by penta-hepta pairs, as in the case of systems of particles undergoing elastic collisions. The left panel of Figure 5 shows the dependence of the geometric order parameter A on η, for both types of collisions. Little difference is observed between the two systems except for $\eta = 0.6$, indicating that, on average, the number of neighbors a particle has in dilute situations is the same for both types of collisions.

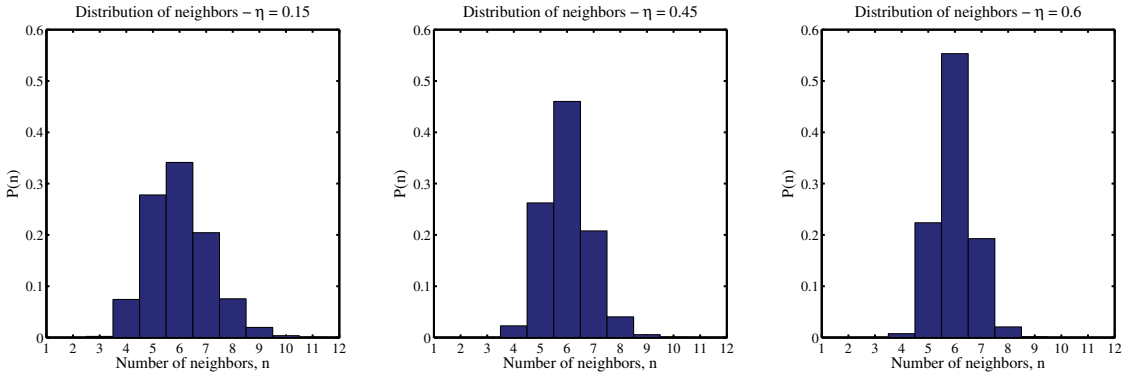

Figure 4. *Probability distribution functions for the number of neighbors of a particle at a given value of the packing fraction η. Left: $\eta = 0.15$, $A = 0.34135$ (variance of A: $\sigma_A^2 = 0.000284$). Middle: $\eta = 0.45$, $A = 0.46020$ ($\sigma_A^2 = 0.000455$). Right: $\eta = 0.60$, $A = 0.55347$ ($\sigma_A^2 = 0.000497$). Each distribution was evaluated by calculating the number of neighbors of each particle at 200 time points (i.e., snapshots) between $t = 50$ and $t = 70$, in a steady state regime of the dynamics. The geometric order parameter A is given by the probability for a particle to have exactly six neighbors, i.e., $A = P(6)$.*

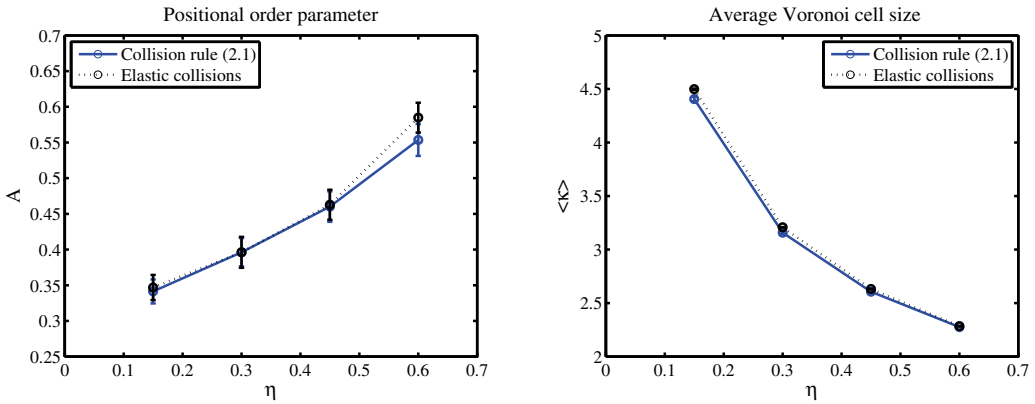

Figure 5. *Geometric order parameter (left) and average Voronoi cell size (right) as functions of the packing fraction η, for both types of collision rules. Error bars correspond to one standard deviation above and below the mean.*

3.2. Distribution of Voronoi cell sizes. The Voronoi tessellation may also be used to calculate the distribution of the surface area of the Voronoi cells. The right panel of Figure 5 shows the average Voronoi cell size $\langle\kappa\rangle$ as a function of η, for both types of collisions. Again, little difference is observed between the two, which is to be expected since in both cases the product $\pi\eta\langle\kappa\rangle^2$ should remain close to 1 when the system has reached steady state (here, this product varies between 9.5 and 1 for collision rule (2.1) and between 9.1 and 1 for elastic collisions). Therefore, average quantities such as the geometric order parameter A and the average Voronoi cell size $\langle\kappa\rangle$ adequately capture the fact that the system becomes increasingly ordered as η increases, but do not differentiate between the two types of collision rules.

However, this difference becomes apparent when one considers probability distributions rather than averaged quantities. As mentioned above, the presence of clusters leads to both

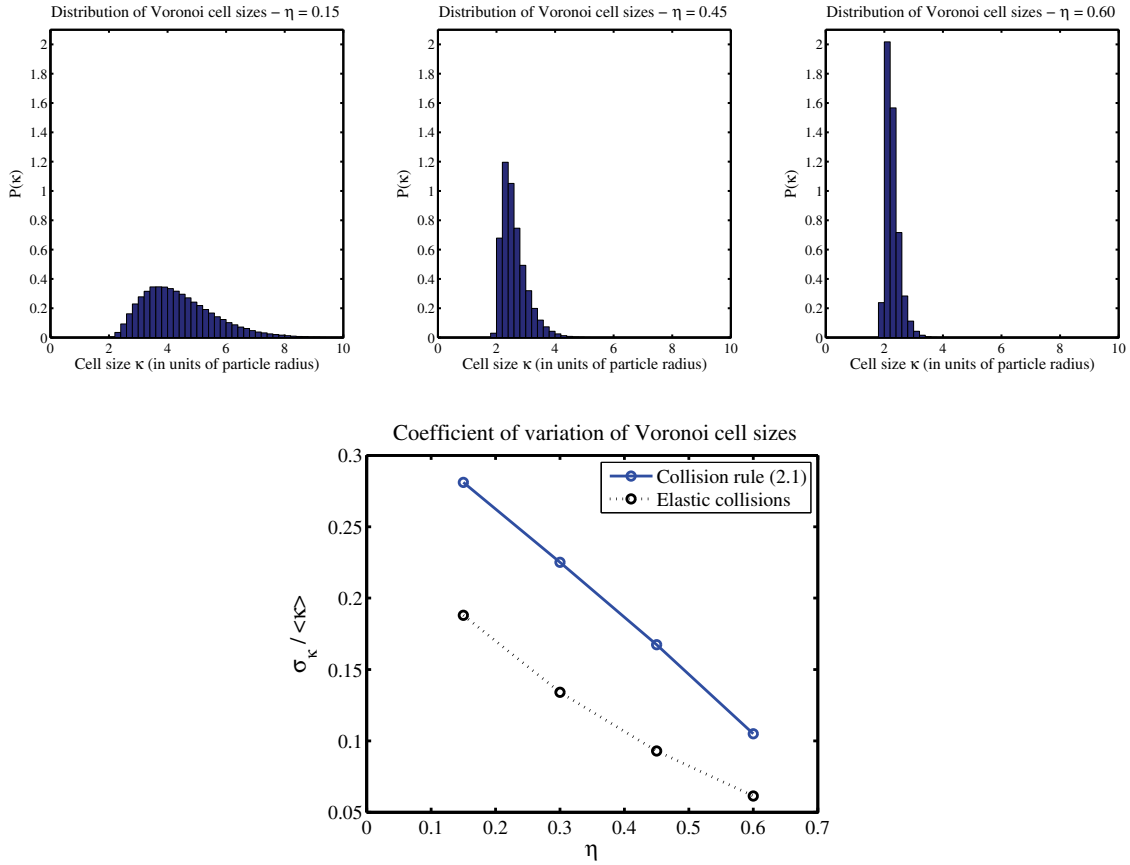

Figure 6. *Probability distribution functions for Voronoi cell sizes κ at a given value of the packing fraction η, and corresponding coefficient of variation. Top left: $\eta = 0.15$ (mean of κ: $\langle\kappa\rangle = 4.4058$, variance of κ: $\sigma_\kappa^2 = 4.2410^{-4}$). Top middle: $\eta = 0.45$ ($\langle\kappa\rangle = 2.6066$, $\sigma_\kappa^2 = 1.7910^{-5}$). Top right: $\eta = 0.60$ ($\langle\kappa\rangle = 2.2764$, $\sigma_\kappa^2 = 2.4310^{-6}$). As before, each distribution was evaluated by computing the Voronoi cell sizes at 200 time points (i.e., snapshots) between $t = 50$ and $t = 70$, in a steady state regime of the dynamics. Bottom row: coefficient of variation of the distribution of Voronoi cell sizes, for both types of collisions.*

large and small Voronoi cells, and therefore a wide distribution of cell sizes. As η increases, the distribution of Voronoi cell sizes narrows, as shown in the top row of Figure 6. It is thus clear that the coefficient of variation $C_\kappa = \sigma_\kappa/\langle\kappa\rangle$ of the distribution of Voronoi cell sizes decreases as a function of η, indicating increased regularity, and therefore order, in the system as the packing fraction gets larger. Figure 6 (bottom row) shows the behavior of C_κ as a function of η for the collision rule described by (2.1) as well as for elastic collisions. Note that for a given value of η, the value of C_κ for rule (2.1) is significantly higher than for elastic collisions, thereby providing a way of quantifying the presence of larger and smaller Voronoi cell sizes in the former case.

We now turn to two other measures of orientational order and clustering, namely, the polarization and the Morisita index.

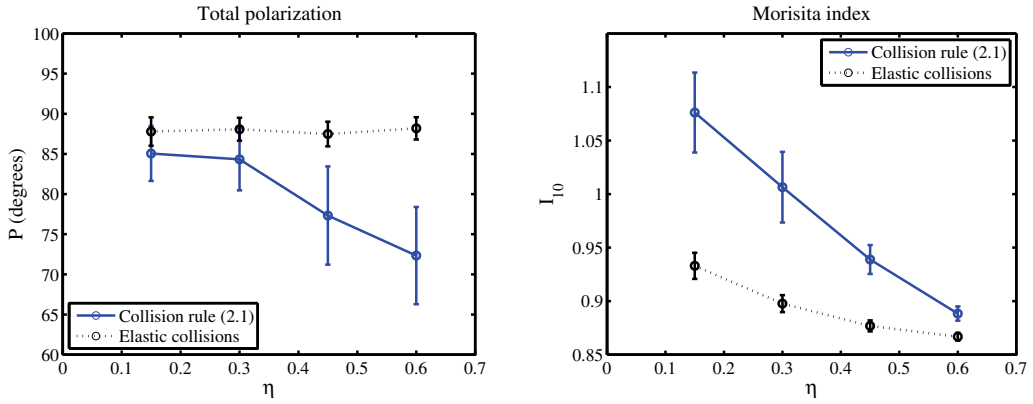

Figure 7. *Left: polarization P. Right: Morisita index. Both quantities are plotted as functions of the packing fraction η, for both types of collision rules. Error bars represent one standard deviation below and above the mean.*

3.3. Polarization. In [10], the polarization p of a group of agents (e.g., fish in a school) is defined as "the average of the angle deviation of each fish to the mean swimming direction of the school. For $p = 0°$ the school is optimally parallel, for $p = 90°$ the school is maximally confused." Here, we define the polarization P as the average of the absolute value of the angle between the direction of motion of each particle and the average direction of motion of the group. In other words,

$$P = \left\langle \sum_{i=1}^{N} |\theta_i(t) - \theta(t)| \right\rangle_t ,$$

where $\langle . \rangle_t$ denotes time averaging, $\theta_i(t) \in [-\pi, \pi]$ is the direction of motion of particle i at time t, and the mean direction of motion $\theta(t)$ is the angle in $[-\pi, \pi]$ such that $\tan(\theta(t)) = \frac{\langle v_y(t) \rangle_N}{\langle v_x(t) \rangle_N}$, where $\langle . \rangle_N$ denotes averaging over all of the particles in the box. A small value of P therefore indicates system-wide coherence of the direction of particle motion. The left panel of Figure 7 shows P (converted to degrees) as a function of η for both types of collisions. Whereas P remains fairly constant in the case of elastic collisions, it decreases as η increases in the case of collision rule (2.1), thereby quantifying the appearance of collective motions in the system.

3.4. Morisita index. The *Morisita index* [53] is often used in statistical ecology (see, for instance, [61]). For a population of N individuals divided into δ units, it is defined as

$$I_\delta = \delta \frac{\sum_{i=1}^{\delta} x_i(x_i - 1)}{N(N-1)},$$

where x_i is the number of individuals in unit i. The Morisita index I_δ thus measures the probability of having any two individuals together in any one of the δ units, divided by that same probability had the individuals been uniformly distributed [53]. In particular, if the units are the cells in a square lattice covering the region where the population is distributed, then I_δ is a good measure of clustering.

Note that if there is at most one particle per cell, then $I_\delta = 0$. This provides a convenient way of checking that particles do not overlap. Indeed, if ρ is the radius of a particle, then

if the box is divided into δ square cells of side length l so that $\sqrt{2}l \leq 2\rho$, then I_δ should be 0 (we consider that a particle is in a given cell if its center of mass falls within that cell). This gives a maximum value for the number of square cells δ used in the numerical box to detect clusters, equal to $\delta_c = \text{floor}(\sqrt{N\pi/(2\eta)})$, where N is the total number of particles in the box. Moreover, all of the numerical simulations presented here are such that I_δ with $\delta = \text{ceil}(\sqrt{N\pi/(2\eta)}) + 1$ is zero; i.e., no overlap between particles is detected.

The right panel of Figure 7 shows the behavior of I_{10} as a function of η for both types of collision rules. Whereas I_{10} decreases moderately as the packing fraction is increased in the case of elastic collisions, it decreases more significantly for the collision rule given in (2.1), thereby picking up, in the latter case, the existence of clusters for small values of η.

In summary, the last three measures indicate significant differences in the behavior of systems with elastic collisions and those described by (2.1). Together, they provide a good quantitative description of the emergence of collective behaviors in systems obeying (2.1), as the packing fraction increases. Although none of these measures would be sufficient to indicate clustering and collective motions by itself, the overall picture obtained by aggregating all of these results confirms that collective behaviors may emerge by altering the collision rule of a collection of hard disks. The next section attempts to provide a measurement of the mean polarization of individual clusters, defined as groups of nearby particles, in systems evolving according to collision rule (2.1).

3.5. Clusters. Clusters of nearby particles were identified with the MATLAB fuzzy c-mean clustering algorithm (`fcm`), assuming that the typical cluster size scales linearly with η. Further processing combined clusters that extensively overlapped. The first row of Figure 8 shows snapshots of the particles and clusters at $t = 65$ for $\eta = 0.15$, $\eta = 0.45$, and $\eta = 0.60$. The clustering algorithm used here gives results that appear reasonable to the eye, but it is not error proof. In particular, clusters can partly overlap, and particles that appear too far apart are sometimes grouped into a cluster. However, in spite of the variability inherent to this procedure, it is interesting to note that for collision rule (2.1), the mean cluster polarization (solid curve in the bottom panel of Figure 8) seems independent of the packing fraction, is relatively low (below 70), and is significantly less than the mean total polarization (dashed curve) of the system, especially for small values of η. This could be interpreted as follows: (i) the tendency of nearby particles (i.e., those in a given cluster) to move together is independent of the packing fraction, and (ii) as the packing fraction increases, the coherence that is observed within small individual clusters is maintained as the clusters become larger. In other words, the mean cluster polarization appears to be a property of the collision rule. In the case of elastic collisions, a similar analysis, with groups of particles of size comparable to that of the clusters identified here, shows that the mean individual cluster polarization remains high, at around 80 or above (dotted curve in Figure 8) for most values of the packing fraction (note the very large error bar for $\eta = 0.15$), indicating a lack of coherence in the motion of nearby particles in dense systems of disks undergoing elastic collisions.

4. Discussion. The work presented here demonstrates, by means of numerical simulations, that collective behaviors may emerge in ensembles of particles that interact *only* through collisions. Note that in these simulations, the particles are not self-propelled, in the sense that the magnitude of their speed is not fixed but is instead a consequence of the initial conditions, the

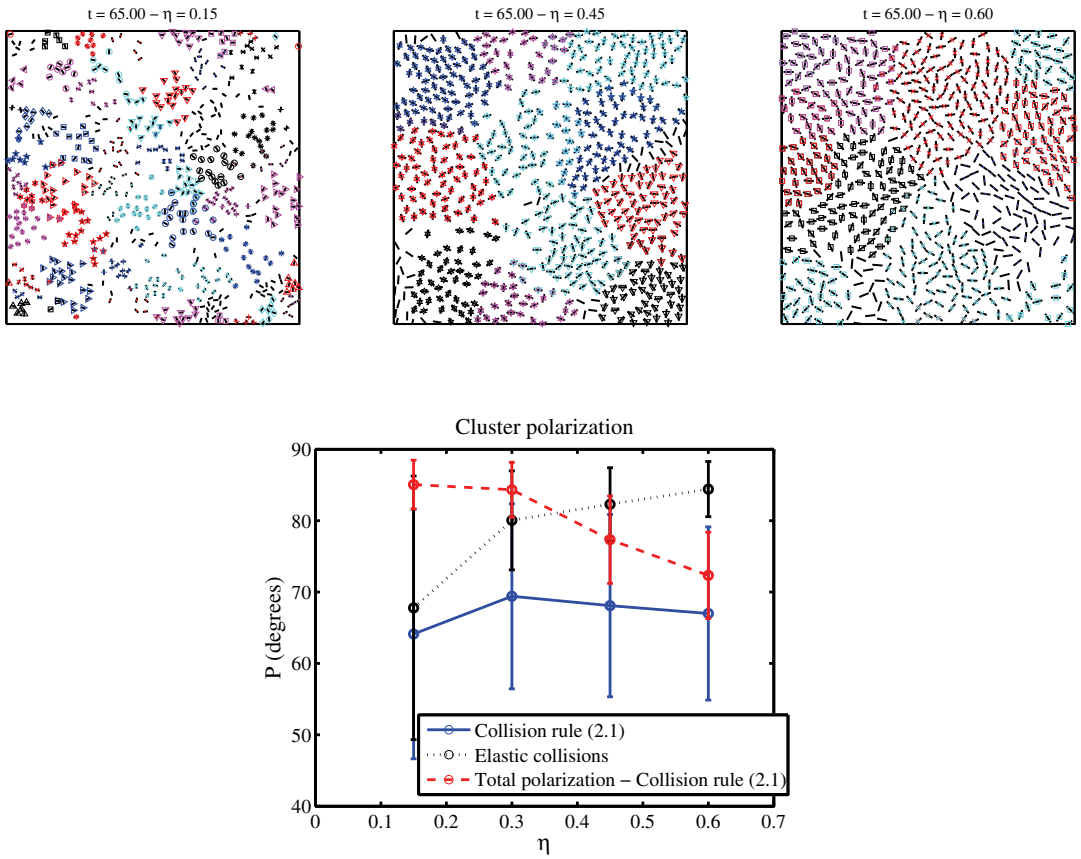

Figure 8. *Top row: output of the clustering algorithm for the snapshots shown in Figure 1. Nearby particles that were identified as belonging to the same cluster are tagged with the same marker. Bottom row: mean cluster polarization as a function of the packing fraction η for both collision rules, together with the total polarization for collision rule (2.1). Error bars represent one standard deviation below and above the mean.*

sequence of collisions undergone by each particle, and the tumbling times. In the steady state regime, the temperature (total kinetic energy) presents very small fluctuations around a value that reflects the balance between the energy lost through collisions and the energy put into the system by the tumbles (since after each tumble, the velocity of the particle is determined from a distribution corresponding to the initial temperature). From a phenomenological point of view, the system described here is close to the system of self-propelled particles described in [28]. In that work, disk-like particles move at constant velocity, undergo random kicks (changes in the direction of their velocity vector following a Gaussian distribution), and collide. The collision rule is such that after each collision, the outgoing directions are obtained by adding Gaussian noise to the direction of the sum of the incoming velocity vectors. In comparison with the present system, the differences are therefore as follows: in [28], (i) random kicks (tumbles) are Gaussian instead of uniformly distributed, (ii) incoming and outgoing velocities have the same magnitude, and (iii) the collision rule lacks the contribution of the transverse term in (2.1) that separates the particles after a collision. As a consequence, it is not clear

whether particles in [28] are prevented from overlapping after a collision. However, it should be possible to extend the Boltzmann equations derived in [28] to the present situation, which might shed some light on the size of the clusters observed at small packing fractions.

We believe our approach to be particularly relevant to the understanding of complex behaviors observed in bacterial systems in which individual bacteria do not seem to communicate, as in the experiments of [42]. The present work may also provide an explanation for the large-scale ordering recently observed in layers of active "granular nematics" [62]. In this case, the active granular nematic consists of copper rods etched at both ends, confined to an almost two-dimensional layer, and vibrated vertically. "Macroscopic swirls," as well as large density fluctuations, are observed in this system [62]. The fact that cylindrical (i.e., not tapered at the ends) rods do not form nematic states [63] may be an indication that the nature of the collisions between the rods plays an important role in the experiments reported in [62]. It is therefore possible that the approach presented here may apply to that work.

Section 3 identifies order parameters that are able to capture the presence of clusters and coherent dynamics in a system of interacting particles. These quantities can be systematically measured in systems of particles obeying various collision rules, and therefore form a collection of tools that can be used to explore the emergence of collective behaviors in different situations.

Even though the particles in this study are disk-like, it does not mean that the results described here apply only to objects that are of circular shape. Along the same lines, the word "collision" does not necessarily mean in this context that the two colliding objects come into contact with one another. Indeed, imagine, for instance, a bacterium that can physically sense the presence of an obstacle in a circular region around its center of mass. The phrase "physically sense" indicates that the sensing is *short-range* and may occur through contact (for instance, if the flagella of the bacterium touch the obstacle) or without contact (for instance, through local hydrodynamic motions of the water in which the bacterium swims). In such a situation, one may be able to define a circular region $\mathcal{R}$ around a rod-like bacterium, such that the bacterium senses the presence of objects when they reach the boundary of $\mathcal{R}$. In the context of this work, such an event would be described as a collision between a disk-like object occupying the region $\mathcal{R}$ and the obstacle.

As mentioned in the introduction, the collision rule used in this work was chosen in a somewhat ad hoc fashion, as a way to interpolate between statements made in [50] and [51]. Since the present work is restricted to two dimensions, the collision rule is such that the colliding particles align their tangential velocities but typically eventually drift apart (since their perpendicular velocities are reversed after the collision). Many recent works describe the interaction of two self-propelled objects moving in a Stokes fluid [51, 64, 65, 66, 67, 68, 69]. Because the flow pattern created by a swimmer in a Stokes fluid typically decays like some power of the inverse of the distance from the swimmer, such interactions are long-range and are believed to be sufficient to explain observed collective behaviors [18]. It may nevertheless be interesting to compile the near-field behaviors that result from these studies in the form of collision rules, and apply them to the present setting. The outcome may of course depend on the type of swimmer used in each work. For instance, rigid dumbbells are considered in [64], squirmers in [65, 66], flagellated ellipsoids in [51], three-sphere swimmers in [67], and spherical and ellipsoidal swimmers in [69]. Performing similar analyses on movies showing how actual bacteria (possibly confined to a thin film as in [70] or on agar plates as in [71]) interact would

also be illuminating. Two very recent articles [72, 73], which describe the flow created by the swimming of two microorganisms, *Volvox carteri* [72] and *Chlamydomonas reinhardtii* [72, 73], are proof that it is now possible to answer such questions experimentally.

The present work does not explain why or how collective behaviors emerge; it simply indicates that such macroscopic phenomena are intrinsically related to the nature of the collision rules that describe the microscopic interaction between particles. We now propose a possible way of mathematically investigating the emergence of such collective behaviors. The appearance of large-scale structures described in section 3 is markedly different from what is observed in a system of hard disks undergoing elastic collisions. The latter is known to be chaotic (see, for instance, [74]), and its Lyapunov spectrum has been numerically shown to exhibit "steps" [75] for small values of the Lyapunov exponents. These steps indicate that the corresponding exponents are degenerate; in particular, the zero exponents reflect the symmetries of the system. It has also been shown that small, nonzero, degenerate exponents are associated with large-scale Lyapunov modes (see [76] for a classification of these modes), also called *Goldstone modes* [77] or *hydrodynamic modes* [78]. (In contrast, the large exponents correspond to localized modes [79].) If it were possible to prevent the growth of the large Lyapunov modes, one would expect to observe the structures associated with the modes of smaller exponents. Because these structures are of macroscopic scale, one would then witness the emergence of collective behaviors. We therefore put forward the idea that the choice of collision rule affects the chaotic nature of (or the "amount of chaos" in) the system, and that an exploration of the Lyapunov spectrum and modes associated with a given collision rule could shed some light on the emergence of collective behaviors. Such an investigation is of course beyond the scope of the present article but will be pursued in future work.

5. Conclusion. This article discusses the emergence of collective behaviors in two-dimensional systems of particles that tumble randomly and collide with their neighbors according to the collision rule given by (2.1). The approach put forward here extends ideas used in the description of animal grouping to a situation where individuals can communicate only at very short range, through collisions. The context of this work is therefore significantly different from that of previous studies because collisions, and therefore interactions between individuals, are localized in time and space. In contrast, the models of animal aggregation discussed in the introduction assume forces that continuously act on the interacting individuals.

We have shown, by means of molecular dynamics simulations, that the new collision rule introduced here leads to the emergence of coherent behaviors in a system with periodic boundary conditions. We have identified order parameters that are able to capture and quantify the formation of coherent structures and have used these quantities to analyze the numerical results. We have also discussed how some of the ideas presented here may be applied to other systems and have proposed a way to investigate the emergence of collective behaviors by analyzing the properties of the Lyapunov spectrum and exponents of the system of interacting particles.

This work was motivated by the experiments on *B. subtilis* described in [42] and fits into the more general framework of the dynamics of complex systems. Bacterial colonies are indeed wonderful examples of multiscale systems and often exhibit very complex dynamics at a variety of scales: the microscopic scale (a few microns) at the level of a bacterium, the mesoscopic scale (tens of microns) at the level of the coherent structures observed in the

system, and the macroscopic scale (a few centimeters) at the level of the colony itself. A macroscopic model for the formation of whirls and jets in a bacterial colony was recently proposed by the author and Passot [80, 81, 82]. This model generalizes reaction-diffusion systems that describe the shape of bacterial colonies by coupling them to a hydrodynamic equation for the mixture of bacteria and water that forms the colony and which is considered as a two-phase fluid. By construction, the model does not capture effects that occur below the scale of a few "bacterial fluid particles"; it also leaves open questions about the nature of the interaction between the bacteria and the fluid they swim in, as well as about the properties of a fluid phase made entirely of bacteria. The present paper considers the problem from the microscopic side. Depending on whether or not the collision rules are mediated by fluid flows, the present approach could describe either a collection of particles interacting in a fluid, or a single-phase fluid in which self-propulsion is replaced by free flight motions at a given (kinetic) temperature.

REFERENCES

[1] W. C. Allee, *Animal aggregations*, Quart. Rev. Biol., 2 (1927), pp. 367–398.
[2] J. K. Parrish and L. Edelstein-Keshet, *Complexity, patterns, and evolutionary trade-offs in animal aggregation*, Science, 284 (1999), pp. 99–101.
[3] A. Okubo, *Dynamical aspects of animal grouping: Swarms, schools, flocks, and herds*, Adv. Biophys., 22 (1986), pp. 1–94.
[4] F. H. Heppner, *Avian flight formations*, Bird Banding, 45 (1974), pp. 160–169.
[5] D. Grünbaum, *Align in the sand*, Science, 312 (2006), pp. 1320–1322.
[6] J. Buhl, D. J. T. Sumpter, I. D. Couzin, J. J. Hale, E. Despland, E. R. Miller, and S. J. Simpson, *From disorder to order in marching locusts*, Science, 312 (2006), pp. 1402–1406.
[7] S. J. McNaughton, *Grazing lawns: Animals in herds, plant form, and coevolution*, Am. Nat., 124 (1984), pp. 863–886.
[8] T. J. Pitcher and B. L. Partridge, *Fish school density and volume*, Marine Biol., 54 (1979), pp. 383–394.
[9] L. Edelstein-Keshet, *Mathematical models of swarming and social aggregation*, invited lecture, The 2001 International Symposium on Nonlinear Theory and Its Applications (NOLTA 2001), Miyagi, Japan; available online at http://www.math.ubc.ca/~keshet/pubs/nolta2001.pdf.
[10] A. Huth and C. Wissel, *The simulation of fish schools in comparison with experimental data*, Ecological Modelling, 75 (1994), pp. 135–145.
[11] H.-S. Niwa, *Newtonian dynamical approach to fish schooling*, J. Theoret. Biol., 181 (1996), pp. 47–63.
[12] A. Mogilner, L. Edelstein-Keshet, L. Bent, and A. Spiros, *Mutual interactions, potentials, and individual distance in a social aggregation*, J. Math. Biol., 47 (2003), pp. 353–389.
[13] Y.-X. Li, R. Lukeman, and L. Edelstein-Keshet, *Minimal mechanisms for school formation in self-propelled particles*, Phys. D, 237 (2008), pp. 699–720.
[14] G. Flierl, D. Grünbaum, S. Levin, and D. Olson, *From individuals to aggregations: The interplay between behavior and physics*, J. Theoret. Biol., 196 (1999), pp. 397–454.
[15] I. D. Couzin, J. Krause, N. R. Franks, and S. A. Levin, *Effective leadership and decision-making in animal groups on the move*, Nature, 433 (2005), pp. 513–516.
[16] B. Nabet, N. E. Leonard, I. D. Couzin, and S. A. Levin, *Leadership in animal group motion: A bifurcation analysis*, in Proceedings of the 17th International Symposium on Mathematical Theory of Networks and Systems, Kyoto, Japan, 2006.
[17] A. Seyfried, B. Steffen, and T. Lippert, *Basics of modelling the pedestrian flow*, Phys. A, 368 (2006), pp. 232–238.
[18] A. Baskaran and M. C. Marchetti, *Statistical mechanics and hydrodynamics of bacterial suspensions*, Proc. Natl. Acad. Sci. USA, 106 (2009), pp. 15567–15572.

[19] T. Vicsek, A. Czirók, E. Ben-Jacob, I. Cohen, and O. Shochet, *Novel type of phase transition in a system of self-driven particles*, Phys. Rev. Lett., 75 (1995), pp. 1226–1229.
[20] H. Levine, W.-J. Rappel, and I. Cohen, *Self-organization in systems of self-propelled particles*, Phys. Rev. E, 63 (2000), 017101.
[21] F. Schweitzer, W. Ebeling, and B. Tilch, *Statistical mechanics of canonical-dissipative systems and applications to swarm dynamics*, Phys. Rev. E, 64 (2001), 021110.
[22] W. Ebeling and F. Schweitzer, *Swarms of particle agents with harmonic interactions*, Theory Biosci., 120 (2001), pp. 207–224.
[23] U. Erdmann, W. Ebeling, and V. S. Anishchenko, *Excitation of rotational modes in two-dimensional systems of driven Brownian particles*, Phys. Rev. E, 65 (2002), 061106.
[24] V. Gazi and K. M. Passino, *Stability analysis of swarms*, IEEE Trans. Automat. Control, 48 (2003), pp. 692–697.
[25] G. Grégoire, H. Chaté, and Y. Tu, *Moving and staying together without a leader*, Phys. D, 181 (2003), pp. 157–170.
[26] G. Grégoire and H. Chaté, *Onset of collective and cohesive motion*, Phys. Rev. Lett., 92 (2004), 025702.
[27] J. Toner, Y. Tu, and S. Ramaswamy, *Hydrodynamics and phases of flocks*, Ann. Physics, 318 (2005), pp. 170–244.
[28] E. Bertin, M. Droz, and G. Grégoire, *Boltzmann and hydrodynamic description for self-propelled particles*, Phys. Rev. E, 74 (2006), 022101.
[29] H.-Y. Chen and K. Leung, *Rotating states of self-propelling particles in two dimensions*, Phys. Rev. E, 73 (2006), 056107.
[30] Y. Chuang, M. R. D'Orsogna, D. Marthaler, A. L. Bertozzi, and L. S. Chayes, *State transitions and the continuum limit for a 2D interacting, self-propelled particle system*, Phys. D, 232 (2007), pp. 33–47.
[31] C. R. McInnes, *Vortex formation in swarms of interacting particles*, Phys. Rev. E, 75 (2007), 032904.
[32] H. Chaté, F. Ginelli, G. Grégoire, and F. Raynaud, *Collective motion of self-propelled particles interacting without cohesion*, Phys. Rev., 77 (2008), 046113.
[33] P. Seiler, A. Pant, and K. Hedrik, *Analysis of bird formations*, in Proceedings of the 41st IEEE Conference on Decision and Control, Vol. 1, 2002, pp. 118–123.
[34] E. Klavins, R. Ghrist, and D. Lipsky, *A grammatical approach to self-organizing robotic systems*, IEEE Trans. Automat. Control, 51 (2006), pp. 949–962.
[35] N. E. Leonard, D. Paley, F. Lekien, R. Sepulchre, D. M. Fratantoni, and R. Davis, *Collective motion, sensor networks, and ocean sampling*, Proc. IEEE, 95 (2007), pp. 48–74.
[36] H. Shi, L. Wang, and T. Chu, *Virtual leader approach to coordinated control of multiple mobile agents with asymmetric interactions*, Phys. D, 213 (2006), pp. 51–65.
[37] R. Olfati-Saber, *Flocking for multi-agent dynamic system: Algorithms and theory*, IEEE Trans. Automat. Control, 51 (2006), pp. 401–420.
[38] A. Videcoq, M. Han, P. Abélard, C. Pagnoux, F. Rossignol, and R. Ferrando, *Influence of the potential range on the aggregation of colloidal particles*, Phys. A, 374 (2007), pp. 507–516.
[39] S. T. Hyde, A. M. Carnerup, A.-K. Larsson, A. G. Christy, and J. M. García-Ruiz, *Self-assembly of carbonate-silica colloids: Between living and non-living forms*, Phys. A, 339 (2004), pp. 24–33.
[40] C. W. Reynolds, *Flocks, herds, and schools: A distributed behavioral model*, Comput. Graphics, 21 (1987), pp. 25–34.
[41] F. Peruani, A. Deutsch, and M. Bär, *Nonequilibrium clustering of self-propelled rods*, Phys. Rev. E, 74 (2006), 030904.
[42] N. H. Mendelson, A. Bourque, K. Wilkening, K. R. Anderson, and J. C. Watkins, *Organized cell swimming motions in Bacillus subtilis colonies: Patterns of short-lived whirls and jets*, J. Bacteriol., 181 (1999), pp. 600–609.
[43] T. Matsuyama and M. Matsushita, *Fractal morphogenesis by a bacterial cell population*, Crit. Rev. Microbiol., 19 (1993), pp. 117–135.
[44] A. Zippelius, *Granular gases*, Phys. A, 369 (2006), pp. 143–158.
[45] I. Goldhirsch and G. Zanetti, *Clustering instability in dissipative gases*, Phys. Rev. Lett., 70 (1993), pp. 1619–1622.

[46] Y. Limon Duparcmeur, H. Herrmann, and J. P. Troadec, *Spontaneous formation of vortex in a system of self motorised particles*, J. Phys. I (France), 5 (1995), pp. 1119–1128.
[47] N. Sambelashvili, A. W. C. Lau, and D. Cai, *Dynamics of bacterial flow: Emergence of spatiotemporal coherent structures*, Phys. Lett. A, 360 (2007), pp. 507–511.
[48] R. M. Macnab, *Flagella*, in *Escherichia coli* and *Salmonella typhimurium*: Cellular and Molecular Biology, F. C. Neidhart, J. L. Ingraham, K. B. Low, M. Schaechter, B. Maganasik, and H. E. Umbarger, eds., American Society for Microbiology, Washington, DC, 1987, pp. 70–83.
[49] H. C. Berg, *Random Walks in Biology*, Princeton University Press, Princeton, NJ, 1993.
[50] I. S. Aranson, A. Sokolov, J. O. Kessler, and R. E. Goldstein, *Model for dynamical coherence in thin films of self-propelled microorganisms*, Phys. Rev. E, 75 (2007), 040901.
[51] T. Ishikawa, G. Sekiya, Y. Imai, and T. Yamaguchi, *Hydrodynamic interactions between two swimming bacteria*, Biophys. J., 93 (2007), pp. 2217–2225.
[52] D. Saintillan and M. J. Shelley, *Orientational order and instabilities in suspensions of self-locomoting rods*, Phys. Rev. Lett., 99 (2007), 058102.
[53] M. Morisita, *Application of the I_δ index to sampling techniques*, Res. Popul. Ecol., 6 (1964), pp. 43–53.
[54] J. M. Haile, *Molecular Dynamics Simulations: Elementary Methods*, John Wiley & Sons, New York, 1992.
[55] M. P. Allen and D. J. Tildesley, *Computer Simulations of Liquids*, Clarendon Press, Oxford, UK, 1987.
[56] D. C. Rapaport, *The Art of Molecular Dynamics Simulation*, 2nd ed., Cambridge University Press, Cambridge, UK, 2004.
[57] B. I. Halperin and D. R. Nelson, *Theory of two-dimensional melting*, Phys. Rev. Lett., 41 (1978), pp. 121–124.
[58] D. R. Nelson and B. I. Halperin, *Dislocation-mediated melting in two dimensions*, Phys. Rev. B, 19 (1979), pp. 2457–2484.
[59] S. Sengupta, P. Nielaba, and K. Binder, *Elastic moduli, dislocation core energy, and melting of hard disks in two dimensions*, Phys. Rev. E, 61 (2000), pp. 6294–6301.
[60] C. H. Mak, *Large-scale simulations of the two-dimensional melting of hard disks*, Phys. Rev. E, 73 (2006), 065104.
[61] E. P. Smith and T. M. Zaret, *Bias in estimating niche overlap*, Ecology, 63 (1982), pp. 1248–1253.
[62] V. Narayan, S. Ramaswamy, and N. Menon, *Long-lived giant number fluctuations in a swarming granular nematic*, Science, 317 (2007), pp. 105–108.
[63] M. van Hecke, *Shape matters*, Science, 317 (2007), pp. 49–50.
[64] J. P. Hernandez-Ortiz, C. G. Stoltz, and M. D. Graham, *Transport and collective dynamics in suspensions of confined swimming particles*, Phys. Rev. Lett., 95 (2005), 204501.
[65] D. Barthès-Biesel, T. Yamaguchi, T. Ishikawa, and E. Lac, *From passive motion of capsules to active motion of cells*, J. Biomech. Sci. Eng., 1 (2006), pp. 51–68.
[66] T. Ishikawa, M. P. Simmonds, and T. J. Pedley, *Hydrodynamic interaction of two swimming model micro-organisms*, J. Fluid Mech., 568 (2006), pp. 119–160.
[67] C. M. Pooley, G. P. Alexander, and J. M. Yeomans, *Hydrodynamic interaction between two swimmers at low Reynolds number*, Phys. Rev. Lett., 99 (2007), 228103.
[68] V. Mehandia and P. R. Nott, *The collective dynamics of self-propelled particles*, J. Fluid Mech., 595 (2008), pp. 239–264.
[69] A. Kanevsky, M. J. Shelley, and A.-K. Tornberg, *Modeling simple locomotors in Stokes flow*, J. Comput. Phys., 229 (2010), pp. 958–977.
[70] X.-L. Wu and A. Libchaber, *Particle diffusion in a quasi-two-dimensional bacterial bath*, Phys. Rev. Lett., 84 (2000), pp. 3017–3020.
[71] H. P. Zhang, A. Beer, E.-L. Florin, and H. L. Swinney, *Collective motion and density fluctuations in bacterial colonies*, Proc. Natl. Acad. Sci. USA, 107 (2010), pp. 13626–13630.
[72] K. Drescher, R. E. Goldstein, N. Michel, M. Polin, and I. Tuval, *Direct measurement of the flow field around swimming microorganisms*, Phys. Rev. Lett., 105 (2010), 168101.
[73] J. S. Guasto, K. A. Johnson, and J. P. Gollub, *Oscillatory flows induced by microorganisms swimming in two dimensions*, Phys. Rev. Lett., 105 (2010), 168102.
[74] G. Gallavotti and E. G. D. Cohen, *Dynamical ensembles in stationary states*, J. Stat. Phys., 80 (1995), pp. 931–970.

[75] Ch. Dellago and H. A. Posch, *Lyapunov instability in a system of hard disks in equilibrium and nonequilibrium steady states*, Phys. Rev. E, 53 (1996), pp. 1485–1501.
[76] J.-P. Eckmann, C. Forster, H. A. Posch, and E. Zabey, *Lyapunov modes in hard-disk systems*, J. Stat. Phys., 118 (2005), pp. 813–847.
[77] A. S. de Wijn and H. van Beijeren, *Goldstone modes in Lyapunov spectra of hard sphere systems*, Phys. Rev. E, 70 (2004), 016207.
[78] M. Mareschal and S. McNamara, *Lyapunov hydrodynamics in the dilute limit*, Phys. D, 187 (2004), pp. 311–325.
[79] C. Forster, R. Hirschl, H. A. Posch, and W. G. Hoover, *Perturbed phase-space dynamics of hard-disk fluids*, Phys. D, 187 (2004), pp. 294–310.
[80] J. Lega and T. Passot, *Hydrodynamics of bacterial colonies: A model*, Phys. Rev. E, 67 (2003), 031906.
[81] J. Lega and T. Passot, *Hydrodynamics of bacterial colonies: Phase diagrams*, Chaos, 14 (2004), pp. 562–570.
[82] J. Lega and T. Passot, *Hydrodynamics of bacteria colonies*, Nonlinearity, 20 (2007), pp. C1–C16.